Turkish J. Eng. Env. Sci.
27 (2003) , 423 – 429.

Thermal Stability of Hydroxylapatite-Titanium and Hydroxylapatite-Titania Composites

Celaletdin ERGUN
İstanbul Technical University, Faculty of Mechanical Engineering,
İstanbul, TURKEY
e-mail: ergunce@itu.edu.tr
Robert H. DOREMUS
Materials Science and Engineering Department,
Rensselaer Polytechnic Institute, Troy, NY 12180 USA
e-mail: doremr@rpi.edu

Received 08.11.2002

Abstract

The aim of the current study is to investigate the reaction of hydroxylapatite with both metallic titanium and titanium oxide, and to examine the effect of atmosphere on these reactions. For this purpose, hydroxylapatite composites with both metallic titanium powder and titanium oxide were prepared and sintered at 1100 °C for 2 h under 2 different conditions: in air and in evacuated glass tubes with hot isostatic pressing at 120MPa. The reaction was monitored with XRD and thermal analysis. No significant reaction was identified between hydroxylapatite and metallic titanium in the vacuum environment. However, a reaction occurred between hydroxylapatite and titanium oxide, which formed $CaTiO_3$ with a perovskite structure, $Ca_3(PO_4)_2$ (whitlockite) and water. The presence of air in the sintering environment promoted this reaction.

Key words: Hydroxylapatite, titanium, biomaterials, implants, interface.

Introduction

Metallic biomaterials such as Ti and its alloys, stainless steel, and CoCrMo alloys are widely used in many load-bearing biomedical applications (Ducheyne *et al.,* 1988; Hemmerle *et al.,* 1997). However, the biocompatibility of these metallic materials has always been an important concern in these applications, in terms of metallic ion release from their surface to the body, and adverse reactions with the surrounding tissue (Ducheyne *et al.,* 1988), etc. Bioceramic materials have been introduced in the biomaterial industry as a solution to this dilemma (Hench *et al.,* 1972; Ducheyne, 1987; Doremus, 1992). Among these bioceramics, calcium phosphate materials have received recognition in this field. Especially hydroxylapatite (HA) among these materials has excellent biocompatibility and direct bond formation with the adjacent hard tissue (Tracy *et al.,* 1984), but its mechanical properties are generally inadequate for many load-carrying applications. Therefore, HA as well as other calcium phosphates are commonly used as a coating material on metallic prostheses; this is perhaps the most salient application of HA currently used (DeGroot *et al.,* 1987; Hemmerle *et al.,* 1997). In this way, hydroxylapatite coatings can also act as a barrier between the body and the metallic implant, and provide a surface on which bone can easily grow, generating mechanical interlocking and chemical bonding at the bone/implant interface (Fujita *et al.,* 1992).

However, the interface between HA and a metallic implant has been another matter of concern in terms of the mechanical properties and biocompatibility of the implant. In order for the HA coating to be effective and reliable, it must be strongly

bonded to the metallic surface. For this reason, chemical bonding derived from the reaction/diffusion at the HA-metal interface could develop a highly reliable interface in response to this requirement (DeGroot *et al.,* 1987). While the presence of reaction/diffusion bonding at the interface may increase the bond strength between HA and the metal, since this new interface material has a different composition from HA or the metal, it may cause toxic reactions in the body. Thus knowledge of the interface phenomena including the reaction kinetics and the properties of byproducts will certainly help to evaluate the overall interface behavior, leading to the design of better implants.

There have been some attempts to understand the interface between HA and metallic substrates, especially titanium. One study documented $CaTi_2O_5$ and tricalcium phosphate formation at the HA/Ti interface as a reaction product in samples prepared with plasma spraying (Ji *et al.,* 1992). Other studies, however, showed $CaTiO_3$ and tricalcium phosphate formation (Geesink *et al.,* 1988; Ji *et al.,* 1992; Ergun *et al.,* 2003). These different reaction products could be due to differences in the sample preparation methods. The aim of the present study is to develop a better understanding of the interface reaction between HA and titanium.

Materials and Methods

Two sets of samples containing hydroxylapatite/metallic Ti powder (HA/Ti) composites in a 3:1 weight ratio and 2 sets of hydroxylapatite/titania (HA/TiO_2) composites also in a 3:1 weight ratio were used to investigate the reaction formation between hydroxylapatite and titanium. The first set of composites was sintered in air to react hydroxylapatite with Ti or TiO_2; the second set was prepared with hot isostatic pressing inside evacuated borosilicate glass tubes. In this case, oxidation was limited. The sample preparations and experimental methods are discussed below.

Preparation of Hydroxylapatite

HA was produced by precipitation (Ergun *et al.*, 2002). First, ammonium phosphate and calcium nitrate solutions were brought to a pH level between 11 and 12, by adding concentrated ammonium hydroxide. These 2 solutions were then covered and stored at room temperature overnight. Next, the calcium nitrate solution was added dropwise to a continually stirred ammonium phosphate solution for 5 to 10 min. The amounts of the 2 solutions were adjusted so that the Ca/P molar ratio in the mixture was 1.67. When all the calcium nitrate solution was exhausted, the slurry was stirred for 3 days. The slurry of the calcium nitrate and ammonium phosphate mixture was then allowed to settle overnight. Following this, the excess liquid was sucked up with a vacuum pump and the settled slurry was filtered using 0.2 μm Millipore filter paper. The wet cakes were dried on plastic film at 60 °C for several days. The dried cakes were first crushed with a mortar and pestle to a particle size below 3 mm, and then further ground to below 200-mesh size.

Preparation of Hydroxylapatite Composites

Hydroxylapatite powder was calcined at 900 °C for 1 h prior to mixing with the other component of the composite. The HA powder was mixed with the powders of metallic titanium or titania so as to give HA/Ti and HA/TiO_2 weight ratios of 3/1. For homogeneous mixing, they were further blended with ball milling in an ethyl alcohol medium. The milled powder was then quickly filtered through a 0.2 μ Millipore filter to prevent segregation due to density differences between the 2 components. The filtered cakes were kept at 200 °C overnight to remove the rest of the the ethyl alcohol. Then the cakes were crushed and further mixed in a mortar and pestle.

Later, the powder was cold-pressed at 120 MPa to produce bar-shaped samples with a 5 mm x 10 mm cross-section and 50-mm length. These green bodies were sintered in 2 different conditions: (a) air sintering; and (b) hot isostatic pressing (HIP).

Table 1. Abbreviation and the composition of the samples.

Name	Abbreviation	Composition
Hydroxylapatite	HA	pure
Hydroxylapatite-metallic Titanium Powder Composite	HA/Ti	75 wt.% HA + 25wt.% Ti
Hydroxylapatite-Titania Composite	HA/TiO_2	75 wt.% HA + 25 wt.% TiO_2

The air sintering was performed at 1100 °C for 2 h. The green bodies prepared for HIP were coated with a boron nitride aerosol spray and dried at 60 °C overnight and were placed into borosilicate glass tubes. The tubes were evacuated with a vacuum pump and sealed with an oxyacetylene torch. The tubes were placed into a graphite supporter and then into the HIP chamber. The chamber was first evacuated to 100 millitorr and heated to 750 °C under vacuum. At this temperature, the chamber pressure was increased to about 20 Pa. Following this stage, it was further heated to 850 °C. At 850 °C, the pressure was increased to 120 MPa over a period of 30 min. Then the temperature and pressure were finally adjusted to 1100 °C and 120 MPa. The samples were HIPped for 2 h. Heating or cooling rates were a maximum of 600 °C/h.

1. Material Characterization

XRD analysis was performed on the pure hydroxylapatite sintered in air at 1100 °C for 2 h, pure TiO_2 in air at 1100 °C for 2 h, commercially available pure Ti powder, and HA/Ti and HA/TiO_2 composites after each processing condition discussed above. The XRD patterns of the pure HA, TiO_2 and Ti were used for comparison purposes to identify the reaction formation and structural changes during processing. An XRD test was run with 2 θ angles between 20 and 70 degrees with 0.02 degree/min scan speed at 40 kV and 30 mA in a Scintag Inc. XRD unit operating with Ni filtered Cu Kα radiation.

The thermal analysis of pure hydroxylapatite and HA/TiO_2 composite samples was conducted in a TA Instruments SDT 2960 TGA system at a 20 °C/min heating/cooling rate from room temperature to 1350 °C under a 100 ml/min air purge.

2. Results and Discussion

The XRD patterns of the HA/Ti composite prepared with HIP can be seen in Figure 1c. When they are compared with the peaks of pure HA, titania, titanium peaks, and whitlockite and perovskite standard peaks in Figures 1a, b, and d-f, respectively, it can be seen that larger amounts of titanium and HA exist in the composite structure when sintered in the vacuum environment, except for a small amount of Ti that oxidized, forming titanium dioxide. It can be presumed that oxygen came from the residual air and/or humidity in the glass tube. It appears that HA and Ti were mainly preserved, and no significant reaction was identified between HA and Ti, as the signals from the reaction products were below the detection limit of the current XRD analysis, which is approximately 0.2%.

The XRD pattern of the HA/Ti composite sintered in air is presented in Figure 2c. The XRD patterns of whitlockite, $Ca_3(PO_4)_2$, and perovskite $CaTiO_3$ standard are also shown in Figures 2a and f. The XRD patterns of the sintered pure HA, sintered rutile TiO_2 and Ti powder as received are given in Figures 1b, d, and e, respectively. The spectrum of the composites includes HA, Ti, $Ca_3(PO_4)_2$and $CaTiO_3$ peaks.

The XRD pattern of the HA/TiO_2 composite prepared with HIP is shown in Figure 3c. The XRD pattern of the sintered pure HA, and sintered titania at 1100 °C can be seen in Figures 3b and d, respectively. The characteristic peaks of the $Ca_3(PO_4)_2$ and $CaTiO_3$are also shown in Figures 4a and e, respectively. The XRD pattern of the composite includes the peaks from rutile titania, HA, and the reaction products: $Ca_3(PO_4)_2$ and $CaTiO_3$.

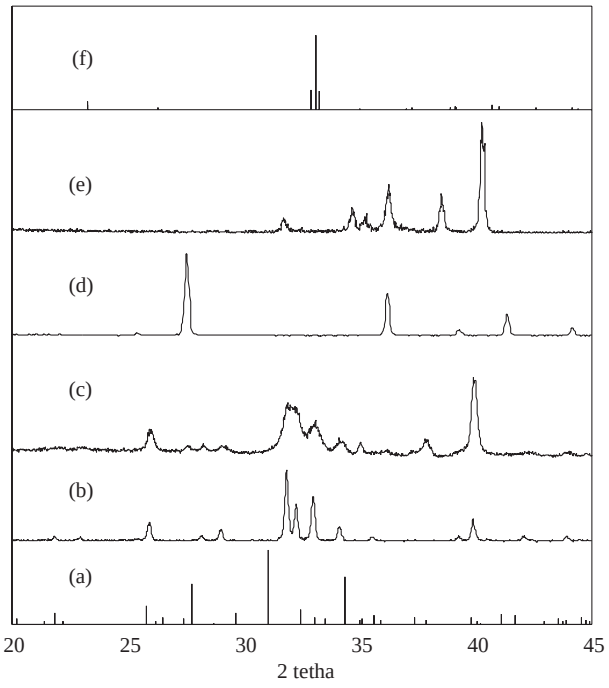

Figure 1. XRD patterns of: (a) JSPD 09-169 standard for $Ca_3(PO_4)_2$ (whitlockite); (b) pure HA; (c) HIPped HA/Ti composite; (d) rutile TiO_2; (e) Ti powder; (f) JSPD 42-0423 standard for $CaTiO_3$ (perovskite).

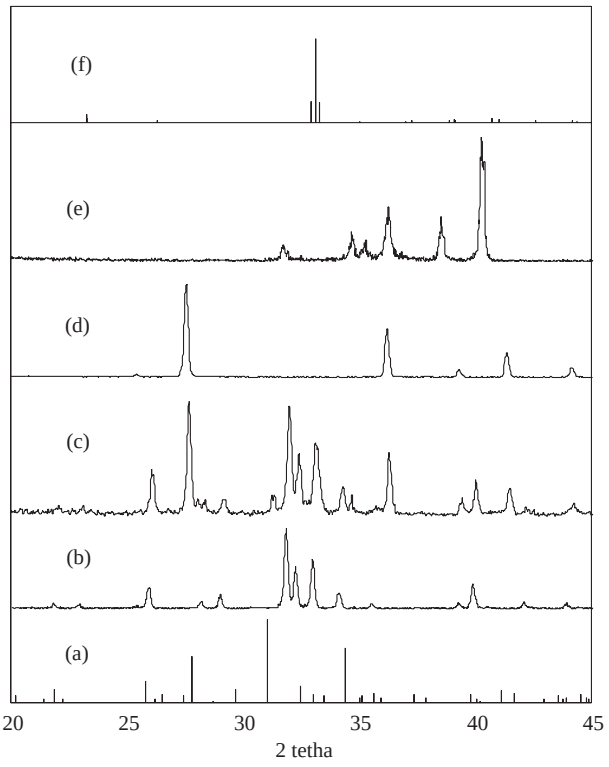

Figure 2. XRD patterns of: (a) JSPD 09-169 standard for $Ca_3(PO_4)_2$ (whitlockite); (b) pure HA; (c) HA/Ti composite sintered in air; (d) rutile TiO_2; (e) Ti powder; (f) JSPD 42-0423 standard for $CaTiO_3$ (perovskite).

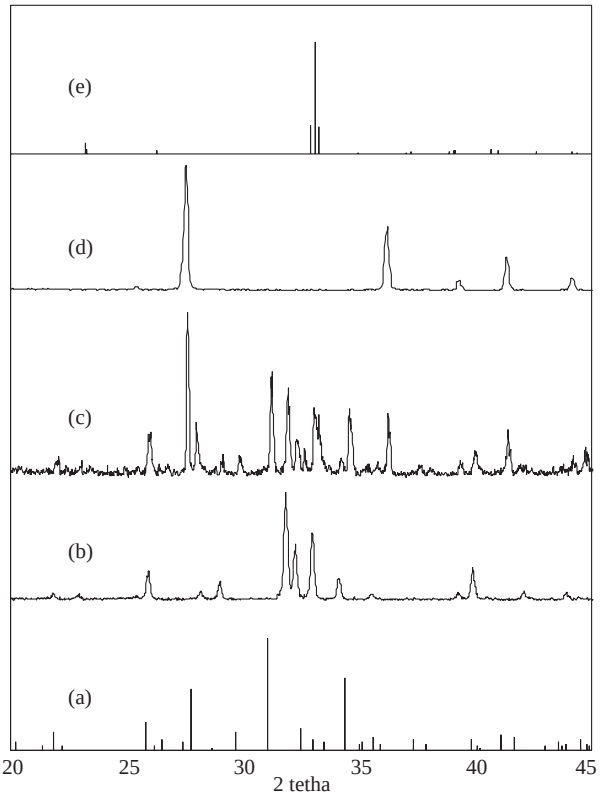

Figure 3. XRD patterns of: (a) JSPD 09-169 standard for $Ca_3(PO_4)_2$ (whitlockite); (b) pure HA; (c) HIPped HA/TiO_2 composite; (d) rutile TiO_2; (e) JSPD 42-0423 standard for $CaTiO_3$ (perovskite).

The XRD pattern of the HA/TiO_2 composite sintered in air is shown in Figure 4c. The XRD patterns of $Ca_3(PO_4)_2$ and $CaTiO_3$ standards are shown in Figures 4a and e. The XRD patterns of the sintered pure HA and sintered rutile (TiO_2) are given in Figure 3b and d, respectively. According to the results, the reactivity of titania with HA is very high, leading to the disassociation of the majority of the HA phase, forming $Ca_3(PO_4)_2$ during the reaction. Another product of this reaction was identified as $CaTiO_3$, similar to that found in the HA/Ti composite sintered in air (Figure 2c).

The TGA and DTA results for pure HA and HA/TiO_2 composite are given in Figures 5 and 6, respectively. According to the TGA results, pure HA loses its absorbed water up to 900 °C. The steps up to this temperature seen in this figure indicate the different release temperatures of the water held with different mechanisms in the structure of HA. It is known that HA contains water in 2 different ways: structural water and absorbed water. The zeolitic structure of the HA having structural channels should be responsible for this excessive water absorption behavior (Sharrock *et al.,* 1992). At about 900 °C, the plot shows a plateau. Its lost weight was about 15-16% of its starting value during heating up to this plateau.

In the DTA graph for HA/TiO_2 composite shown in Figure 6, a strong endothermic peak was observed at about 960 °C. This temperature showed a good correlation with the temperature at which a weight loss of the HA/TiO_2 composite was observed in the TGA plot in Figure 5. The weight loss observed in the TGA plot at 960 °C can be attributed to the evaporation of the water released from the structure after the reaction between HA and TiO_2.

According to these results, HA reacts with titania at approximately 960 °C in air, and validates the following reaction proposed by Geesink *et al.* (1988) and Ergun *et al.* (2003):

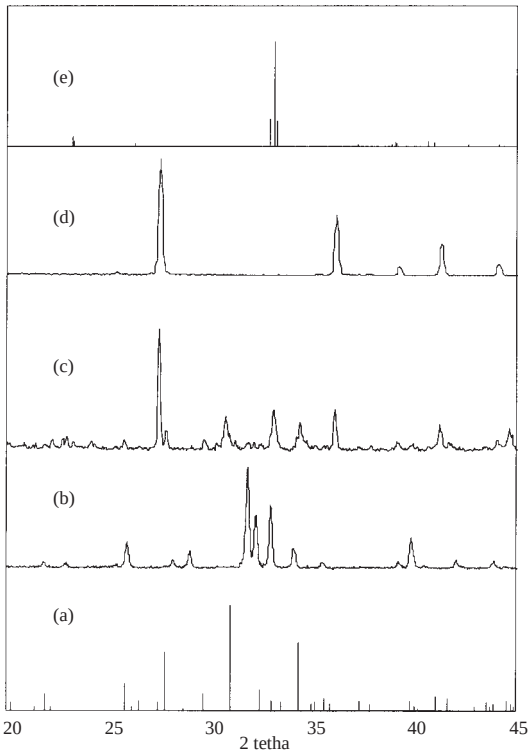

Figure 4. XRD patterns of: (a) JSPD 09-169 standard for $Ca_3(PO_4)_2$ (whitlockite); (b) pure HA; (c) HA/TiO_2 composite sintered in air; (d) rutile TiO_2; (e) JSPD 42-0423 standard for $CaTiO_3$ (perovskite).

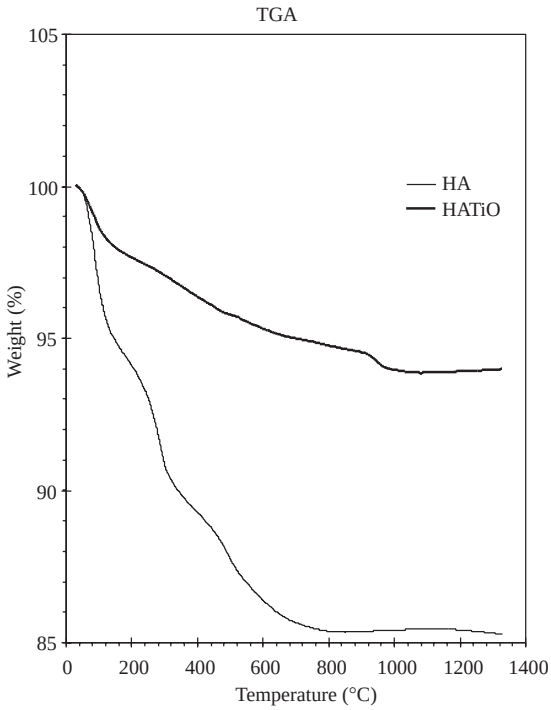

Figure 5. TGA plots of pure HA and HA/TiO_2 composite (HATiO).

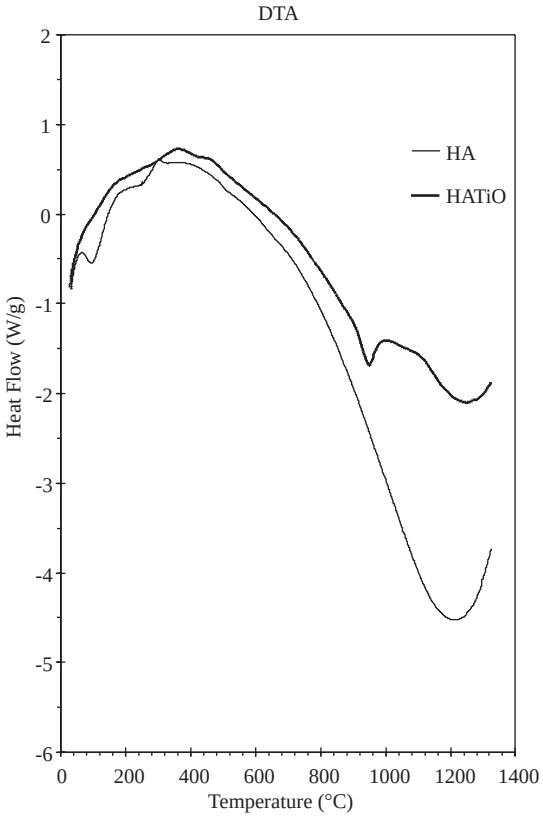

Figure 6. DTA plots of pure HA and HA/TiO_2 composite (HATiO).

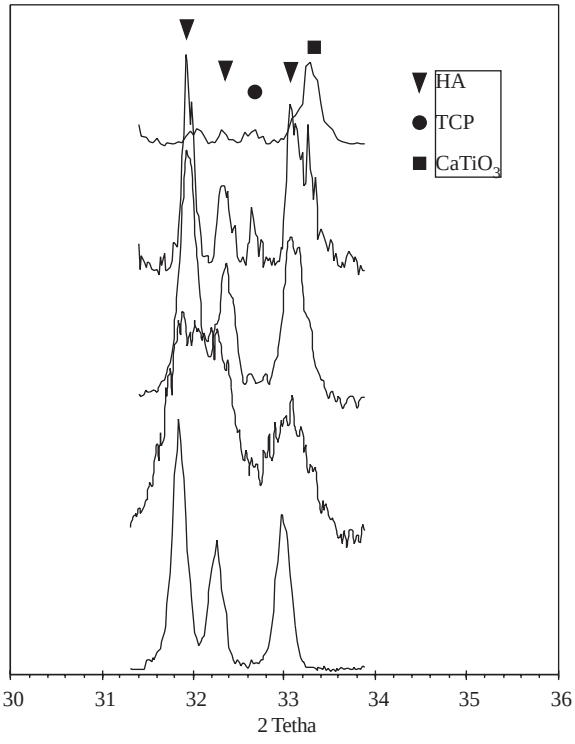

Figure 7. XRD patterns of: (a) pure HA; (b) HIPped HA/Ti composite; (c) HA/TiO_2 composite sintered in air; (d) JSPD 42-0423 standard for $CaTiO_3$ (perovskite).

$Ca_{10}(PO_4)_6(OH)_2 + TiO_2 \Rightarrow CaTiO_3 + 3Ca_3(PO_4)_2 + H_2O$

XRD patterns of pure HA, HIPped HA/Ti composite, HA/Ti composite sintered in air, HIPped HA/TiO_2 composite, and HA/TiO_2 composite sintered in air are shown in Figures 7a-e respectively, to summarize $CaTiO_3$formation for different processing conditions. The intensity ratio of the characteristic XRD peaks of $CaTiO_3$ at 33.41 degrees and HA at 31.77 degrees were estimated as 14/20 for HIPped HA/TiO_2 composite, and 11/2 for HA/TiO_2 composite sintered in air. It is clearly seen that there is a higher reactivity between HA and TiO_2 sintered in air compared to the reactivity between HA and TiO_2 under HIP. This is likely due to the air in the heating environment. However, no reaction was identified between HA and metallic titanium in the HIPped condition. The reaction observed in the air sintered HA/Ti composite appears to be due to the oxidation of the metallic titanium forming titanium dioxide, and then the reaction of this oxide with hydroxylapatite.

3. Conclusion

This study showed that a chemical reaction between titania and hydroxylapatite takes place upon heating at 960 °C. DT analysis supplied evidence that hydroxylapatite decomposed to $Ca_3(PO_4)_3$ and H_2O at this temperature and reacted with titania forming $CaTiO_3$. No direct reaction was observed between titanium and HA. However, it is apparent that the titanium oxide layer reacted with HA. Titanium oxide could have been on the surface of the metallic titanium previously and/or have been formed by the oxidation of titanium. The reactivity between HA and titania increases as the amount of air increases in the processing environment.

References

DeGroot, K., Geesink, R., Klein, C.P.A.T. and Serekian, P. "Plasma Sprayed Coating of Hydroxylapatite", Journal of Biomedical Material Research 21, 1375-1381, 1987.

Doremus, R.H. "Bioceramics". Journal of Materials Science 27, 285-297, 1992.

Ducheyne, P. "Bioceramics: Material Characteristics versus In-vivo Behavior". Journal of Biomedical Material Research: Applied Biomaterials 21A, 219-236, 1987.

Ducheyne, P. and Healy, K.E. "The Effect of Plasma Sprayed Calcium Phosphate Ceramic Coatings on the Metal Ion Release from Porous Titanium and Cobalt-Chromium Alloys". Journal of Biomedical Material Research 22, 1137-1163, 1988.

Ergun, C., Doremus, R.H. and Lanford, W.A., "Hydroxylapatite-Titanium Interfacial Reactions", Journal of Biomedical Material Research 65A, 336-343, 2003.

Ergun, C., Webster, T.J., Doremus, R.H. and Bizios, R. "Hydroxylapatite with Substituted Mg, Zn, Cd, and Y: I Structure and Microstructure". Journal of Biomedical Material Research 59, 305-311, 2002.

Fujita, Y., Yamamuro, T., Nakamura, T., Kitsugi, T., Kotani, S., Ohtsuki, C. and Kokubo, T. "Mechanisms and Strength of Bonding Between Two Bioactive Ceramics *in vivo*", Journal of Biomedical Material Research 26, 1311-1324, 1992.

Geesink, R., De Groot, K. and Klein, C.P.A.T. "Bonding of Bone to Apatite-Coated Implants". Journal of Bone and Joint Surgery 70-B, 17-22, 1988.

Hemmerle, J., Oncag, A. and Erturk, S. "Ultrastructural Features of the Bone Response to Plasma Sprayed in Sheep". Journal of Biomedical Material Research 36, 418-425, 1997.

Hench, L.L., Splinter, R.J., Allen, W.C. and Greenleen Jr., T.K. "Bonding Mechanisms at the Interface of Ceramic Prosthetic Materials". Journal of Biomedical Material Research. 2, 117-141, 1972.

Ji, H., Ponton, C.B. and Marquise, P.M., "Microstructural Characterization of Hydroxylapatite Coating on Titanium". Journal of Materials Science: Materials in Medicine. 3, 283-287, 1992.

Sharrock P. and Bonel G. "Color Centers in Plasma-Sprayed Hydroxylapatite". Biomaterials 13, 755-757, 1992.

Tracy, B.M. and Doremus, R.H. "Direct Electron Microscopy Studies of the Bone Hydroxylapatite Interface", Journal of Biomedical Material Research 18, 719-726, 1984.